Published in final edited form as:
Pharmacol Res. 2011 October ; 64(4): 359–363. doi:10.1016/j.phrs.2011.07.001.

The ABC membrane transporter ABCG2 prevents access of FAAH inhibitor URB937 to the central nervous system

Guillermo Moreno-Sanz[a,b], **Borja Barrera**[c,d], **Ana Guijarro**[a], **Ilaria d'Elia**[a], **Jon Andoni Otero**[c,d], **Ana I Alvarez**[c,d], **Tiziano Bandiera**[b], **Gracia Merino**[c], and **Daniele Piomelli**[a,b,*]

[a]Departments of Pharmacology and Biological Chemistry, University of California, Irvine, 360 MSRII, Irvine, CA, 92697, USA

[b]Drug Discovery and Development, Italian Institute of Technology, via Morego 30, Genoa, Italy, 16163

[c]INDEGSAL, Campus Vegazana s/n, University of Leon, 24071 Leon, Spain

[d]Department of Biomedical Sciences -Physiology, Veterinary Faculty, Campus Vegazana s/n, University of Leon, 24071 Leon, Spain

Abstract

The *O*-arylcarbamate URB937 is a potent inhibitor of fatty-acid amide hydrolase (FAAH), an intracellular serine hydrolase responsible for the deactivation of the endocannabinoid anandamide. URB937 is unique among FAAH inhibitors in that is actively extruded from the central nervous system (CNS), and therefore increases anandamide levels exclusively in peripheral tissues. Despite its limited distribution, URB937 exhibits marked analgesic properties in rodent models of pain. Pharmacological evidence suggests that the extrusion of URB937 from the CNS may be mediated by the ABC membrane transporter ABCG2 (also called Breast Cancer Resistance Protein, BCRP). In the present study, we show that URB937 is a substrate for both mouse and human orthologues of ABCG2. The relative transport ratios for URB937 in Madin-Darby canine kidney (MDCKII) cells monolayers over-expressing either mouse Abcg2 or human ABCG2 were significantly higher compared to parental monolayers (13.6 and 13.1 vs 1.5, respectively). Accumulation of the compound in the luminal/apical side was prevented by co-administration of the selective ABCG2 inhibitor, Ko-143. *In vivo* studies in mice showed that URB937 (25 mg-kg^{-1}) readily entered the brain and spinal cord of Abcg2-deficient mice following intraperitoneal administration, whereas the same dose of drug remained restricted to peripheral tissues in wild-type mice. By identifying ABCG2 as a transport mechanism responsible for the extrusion of URB937 from the CNS, the present results should facilitate the rational design of novel peripherally restricted FAAH inhibitors.

*Corresponding author: Daniele Piomelli, PhD Department of Pharmacology, University of California, Irvine, 360 MSRII, Irvine, CA, 92697, USA Fax: (39) 010-7170187 piomelli@uci.edu.

There are no conflicts of interest.

Keywords

Fatty-acid amide hydrolase; URB937; Breast cancer resistance protein; blood-brain barrier; central nervous system; Abcg2-deficient mice

1. Introduction

The intracellular hydrolysis of the endocannabinoid anandamide is catalyzed by the enzyme fatty-acid amide hydrolase (FAAH) [1], a membrane-bound serine hydrolase that also catalyzes the cleavage of other non-cannabinoid fatty-acid amides such as oleoylethanolamide and palmitoylethanolamide [1–2]. The *O*-arylcarbamate URB937 (cyclohexylcarbamic acid 3'-carbamoyl-6-hydroxybiphenyl-3-yl ester; also referred to as ARN354) is a potent and selective FAAH inhibitor. Following systemic administration in mice, URB937 inhibits liver FAAH activity with a half-maximal effective dose (ID_{50}) of 0.1 mg-kg^{-1}, but fails to alter FAAH activity in forebrain, hypothalamus and spinal cord. Furthermore, *in vivo* inhibition of FAAH by URB937 is accompanied by an elevation of anandamide levels, which occurs exclusively in peripheral tissues. Despite its restricted access to the central nervous system (CNS), URB937 exerts profound antinociceptive effects in rodent models, which are prevented by blockade of CB_1 cannabinoid receptors [3]. Pharmacological evidence suggests that the extrusion of URB937 from the mouse brain may be mediated by ABCG2 (Breast Cancer Resistance Protein, BCRP), a member of the ATP-binding cassette (ABC) superfamily of efflux transporters. ABCG2 was first identified in 1998 in the multidrug resistant human breast cancer cell line MCF-7/AdrVp [4]. ABCG2 can transport a large number of structurally unrelated compounds and is increasingly recognized for its role in drug disposition and tissue protection [5–6]. ABCG2 is highly expressed in organs that are important for the absorption (small intestine), elimination (liver and kidney), and distribution (blood-brain and placental barriers) of drugs and other xenobiotics [7]. Despite its substantial medical significance, the transport mechanism of ABCG2 remains poorly understood.

In the present study, we used both *in vitro* and *in vivo* approaches to examine whether ABCG2 mediates the transport of URB937 and its extrusion from the CNS. We measured the transport rate of URB937 through polarized monolayers of Madin-Darby canine kidney (MDCK II) cells that over-express either mouse Abcg2 or human ABCG2. The effect of Ko143, a selective ABCG2 inhibitor [8], was also assessed. Additionally, we used Abcg2-deficient (Abcg2$^{-/-}$) mice to further explore the role of ABCG2 in the distribution of URB937.

2. Materials and methods

2.1. Animals

Adult male Swiss-Webster mice (25–30 g) and adult male Abcg2$^{-/-}$ mcie and wild-type littermates (9–13 weeks, >99% FVB genetic background) were kept in a temperature-controlled environment with a 12-h light/12-h dark cycle and received a standard chow and water *ad libitum.* Abcg2$^{-/-}$ mice were kindly provided by Dr. A.H. Schinkel, Netherlands Cancer Institute (Amsterdam, The Netherlands). All procedures met the National Institutes of Health guidelines for the care and use of laboratory animals and the “Principles of Laboratory Animal Care” and the European guidelines described in the EC Directive 86/609. Procedures were also approved by the Institutional Animal Care and Use Committee of the University of California, Irvine, and the Research Committee of Animal Use of the University of León (Spain).

2.2. Chemicals

Ko143 was purchased from Tocris (Bristol, UK), isoflurane (Isovet®) from Schering-Plough (Madrid, Spain), anandamide-[ethanolamine-^{3}H] (10,000 cpm, specific activity 60 Ci/mmol) from American Radiolabeled Chemicals (St. Louis, MO, USA). URB937 was synthesized as described [3]. All other chemicals were of analytical grade and available from commercial sources.

2.3. Cell cultures

MDCKII cells and their human ABCG2- and murine Abcg2-transduced subclones were a kind gift of Dr. A.H. Schinkel. Culture conditions were as previously described [9–10]. The cells were cultured in Dulbecco-Modified Eagles's Medium (DMEM) supplemented with Glutamax (Life Technologies, Inc., Carlsbad, CA, USA), penicillin (50 units/ml), streptomycin (50 μg/ml), and 10% (v/v) fetal calf serum (MP Biomedicals, Solon, OH, USA). Cells were cultured at 37°C in the presence of 5% CO_2. Cells were trypsinized every 3 to 4 days for subculturing.

2.4. Transport studies

Transepithelial transport assays were carried out using Transwell plates as previously described [11], with minor modifications. Cells were seeded on microporous polycarbonate membrane filters (3.0 μm pore size, 24 mm diameter; Transwell 3414; Costar, Corning, NY) at a density of 1.0×10^6 cells per well. Cells were grown for 3 days, and the medium was replaced every day. Transepithelial resistance was measured in each well using a Millicell ERS ohmmeter (Millipore, Bedford, MA); wells registering a resistance of 150 ohms or greater, after correcting for the resistance obtained in blank control wells, were used in transport experiments. The measurements were repeated at the end of the experiment to check the tightness of the monolayer. Two hours before the start of the experiment, medium on both sides of the monolayer was replaced with 2 ml of Optimem medium (Life Technologies, Inc., Carlsbad, CA, USA), without serum, either with or without Ko143 (1 μM). The experiment was started (t = 0) by replacing the medium in either the apical or basolateral compartment with fresh Optimem medium, either with or without Ko143 (1 μM), and containing 5 μM URB937. Aliquots of 100 μL were taken from the drug opposite compartment at t = 2 and 4 h, and stored at –20 °C until analysis. The appearance of the compound in the acceptor compartment is presented as fraction of total compound added to the donor compartment at the beginning of the experiment. Active transport across MDCKII monolayers was expressed by the relative transport ratio, defined as the percentage apically directed transport divided by the percentage basolaterally directed translocation, after 4 h [12]

2.5. Tissue processing

Animals were killed by decapitation under slight anesthesia with isoflurane and brain, spinal cord, liver and kidney tissue were snap frozen in liquid nitrogen. Blood was collected through a left cardioventricular puncture and centrifuged at 2000 × *g* for 30 min to obtain plasma. Samples were weighed and homogenized in ice-cold Tris–HCl buffer (50 mM, 5–9 vol., pH 7.5) containing 0.32 M sucrose. Homogenates were centrifuged at 1000 × *g* for 10 min at 4°C. Supernatants were collected (250 μl) and protein concentration determined using a bicinchoninic acid (BCA) assay kit (Pierce, Rockford, IL, USA). Remaining supernatant and pellet where further extracted with methanol/chloroform for URB937 analysis.

2.6. FAAH activity

FAAH activity was measured at 37°C for 30 min in 0.5mL of Tris-HCl buffer (50 mM, pH 7.5) containing fatty acid-free bovine serum albumin (BSA) (0.05%, w/v), tissue

homogenates (50 μg protein from brain, spinal cord and kidney and 100 μg from liver), 10 μM anandamide, and anandamide-[ethanolamine-^{3}H] (10,000 cpm, specific activity 60 Ci/mmol; American Radiolabeled Chemicals). The reactions were stopped with chloroform/methanol (1:1, 1 mL) and radioactivity was measured in the aqueous layers by liquid scintillation counting.

2.7. Lipid extraction and URB937 quantification by liquid chromatography/mass spectrometry (LC/MS)

Tissue and plasma levels of URB937 were determined as previously described [3] with minor modifications. In brief, aqueous tissue homogenates and plasma samples were extracted with methanol/chloroform (1:2) containing cyclohexyl biphenyl-3-ylacetamide as internal standard.

Organic phases were evaporated under nitrogen and reconstituted in 60 μL of methanol. Samples were analyzed using an 1100-LC system coupled to a 1946A-MS detector (Agilent Technologies, Inc., Palo Alto, CA) equipped with an electrospray ionization interface. URB937 and *N*-cyclohexyl biphenyl-3-ylacetamide (mass-to-charge ratio, m/z = 377 and 294 respectively) were eluted on an XDB Eclipse C18 column (50×4.6mm inner diameter, 1.8 μm, Zorbax) using a linear gradient of 60% to 100% of A in B over 3 min at a flow rate of 1.0 mL/min. Mobile phase A consisted of methanol containing 0.25% acetic acid and 5 mM ammonium acetate; mobile phase B consisted of water containing 0.25% acetic acid and 5 mM ammonium acetate.

2.8. Experimental design for *in vivo* studies

URB937 was dissolved in saline/PEG400/Tween-80 (18:1:1) to a concentration of 2.5 mg-mL^{-1} and injected subcutaneously between the shoulder blades at the volume of 10 mL-kg^{-1} for a final dosing of 25 mg-kg^{-1}.

2.8.1. Effects of ABCG2 blockade on URB937 penetration in the brain—Sixteen Swiss-Webster male mice were randomly divided into 4 groups, each receiving a single dose of Ko143 (0, 1, 3 and 10 mg-kg^{-1}, i.p.;10 mL-kg^{-1}) dissolved in saline/PEG400/Tween-80 (18:1:1) with DMSO (30%), 20 min prior to URB937 administration. Animals were killed 1 h later and brains were collected for URB937 levels and FAAH activity determination.

2.8.2. Distribution of URB937 in Abcg2-deficient mice (Abcg2$^{-/-}$)—Wild-type (n = 5) and Abcg2$^{-/-}$ mice (n = 4) received a single dose of URB937 (25 mg-kg^{-1}, subcutaneous, s.c.) and killed after 1 h for tissue collection.

2.9. Statistical analysis

Results are expressed as mean ± standard error of the mean (S.E.M.) or standard deviation (S.D.) and the significance of differences was determined using one-way analysis of variance (ANOVA) followed by Dunett test as *post hoc*, and Student's *t*-test. Differences were considered significant if $P < 0.05$. Statistical analyses were conducted using GraphPad Prism Version 4.0 (San Diego, CA, USA).

3. Results

3.1. Effects of ABCG2 blockade on URB937 penetration in the brain

Systemic administration of the selective ABCG2 inhibitor, Ko143 (0, 1, 3 and 10 mg-kg^{-1}, i.p.), 20 min prior to injection of URB937 (25 mg-kg^{-1}, s.c.), dose-dependently increased access of URB937 to the brain (Fig. 1a). The elevation in brain URB937 levels was

accompanied by a dose-dependent decrease in brain FAAH activity (Fig. 1b), which was assessed *ex vivo* 1 h after URB937 administration. These results confirm and extend previous observations suggesting that pharmacological blockade of ABCG2 activity allows URB937 to enter the CNS [3].

3.2. Transcellular transport of URB937 in vitro

To assess whether URB937 is a substrate for Abcg2/ABCG2, we investigated the polarized transport of this compound using wild-type MDCKII cells as well as MDCKII sub-clones stably over-expressing either mouse Abcg2 or human ABCG2. Relative transport ratios for URB937 were significantly increased in Abcg2 and ABCG2-transduced MDCKII cells, compared to parental cells (Fig.2a, b and c). Inclusion on the incubations of the ABCG2 inhibitor Ko143 (1 μM), completely inhibited Abcg2/ABCG2-mediated transport (Fig. 2d, e and f). These findings indicate that URB937 is an *in vitro* substrate for both the mouse and human orthologues of ABCG2.

3.3. Distribution of URB937 in Abcg2$^{-/-}$ mice

To further examine the role of Abcg2 in the peripheral segregation of URB937, we administered the compound (25 mg-kg^{-1}, s.c.) to Abcg2$^{-/-}$ mice and their wild-type littermates. There were no differences between wild-type and mutant mice in either circulating levels of URB937 (Table 1) or tissue-to-blood ratio (liver and kidney, Fig. 3a). However, levels of URB937 in brain and spinal cord, two organs protected by the blood-brain barrier, were substantially higher in mice lacking Abcg2 (Fig. 3b). Consistent with those findings, Abcg2$^{-/-}$ mice displayed a marked reduction (80%) in FAAH activity in brain and spinal cord compared to wild-type animals, which showed almost no inhibition of FAAH activity in CNS (Fig. 3c). On the other hand, FAAH activity was nearly abolished in liver and kidney tissue in wild-type and Abcg2$^{-/-}$ mice (Fig. 3c). These findings provide conclusive evidence that Abcg2 restricts the access of URB937 to the mouse CNS *in vivo*.

4. Discussion

The *O*-arylcarbamate URB937 is a potent and selective inhibitor of intracellular FAAH activity. In rodents, systemic administration of URB937 inhibits FAAH and elevates anandamide levels in peripheral tissues, but not in forebrain, hypothalamus or spinal cord. Indeed, URB937 is 400 times more potent at inhibiting FAAH activity in mouse liver than in mouse brain [3]. Despite its peripheral distribution, URB937 exerts substantial analgesic effects in mice and rats, which are dependent on CB_1 receptor activation. Previous pharmacological experiments have suggested that the extrusion of URB937 from brain might be mediated by the ABC-transporter ABCG2 [3]. In the present study, we tested this hypothesis utilizing both *in vitro* and *in vivo* approaches. First, we used the polarized canine kidney cell line MDCKII and its subclones transduced with murine Abcg2 and human ABCG2 cDNAs to determine whether URB937 interacts with ABCG2 *in vitro*. Cells were grown to confluent polarized monolayers on porous membrane filters, and vectorial transport of URB937 across the monolayers was assessed. In general, Abcg2/ABCG2 substrates show a higher relative transport ratio in the Abcg2/ABCG2 transduced cells compared to the parental cells due to both heightened transport to the apical side and diminished transport to the basolateral side. Our results show that the relative transport ratio for URB937 was increased nearly 10 folds by over-expression of either mouse or human ABCG2. This effect was prevented by the addition of the selective ABCG2 inhibitor, Ko143. We interpret these findings to indicate that URB937 is an *in vitro* substrate for ABCG2.

To further investigate the role of ABCG2 in the extrusion of URB937, we examined the distribution of this compound in Abcg2$^{-/-}$ mice and their wild-type littermates. Irrespective of genotype, URB937 abrogated FAAH activity in peripheral tissues. By contrast, the drug strongly inhibited FAAH activity in the CNS of Abcg2$^{-/-}$ mice, but failed to do so in wild-type mice. CNS levels and tissue/blood ratio of URB937 were also significantly increased in Abcg2$^{-/-}$ mice. Together with our in vitro data, these results indicate that ABCG2 restricts the access of URB937 to the CNS, without affecting plasma levels or peripheral tissue distribution of this compound.

This interpretation is consistent with several studies reporting local effects mediated by Abcg2, including brain penetration, but no differences in systemic profiles between wild-type and Abcg2$^{-/-}$ mice [13–16]. Although URB937 is an *in vitro* substrate for Abcg2, additional factors could affect the systemic disposition of this compound due to profound differences in tightness and drug uptake systems between systemic membranes and the blood-brain barrier endothelial luminal membrane [16]. Hence, the relevance of ABCG2 for brain penetration of any given substrate will depend upon other constituents of the blood–brain barrier [17]. Among these, the ABC transporter P-glycoprotein (Pgp/ABCB1) is known to overlap with ABCG2 in substrate specificity [16]. By using Abcg2$^{-/-}$ mice in which Pgp is still present, it could be difficult to unequivocally demonstrate a functional role for Abcg2 at the blood-brain barrier [18]. However, in our study, we could demonstrate the role of ABCG2 in the brain extrusion of URB937 together with a difference in FAAH activity depending on murine genotype. The role of P-glycoprotein in this process is currently under investigation.

Preliminary structure-activity relationship explorations suggest that the *para*-hydroxyl substituent in the proximal ring of URB937 is a key determinant of the constrained brain penetration of this compound [3]. The importance of the phenol moiety raises the question as to whether phenol sulfotransferases (SULT1) might be involved in the extrusion of URB937 from the CNS. ABC-transporters commonly co-localize with sulfotransferases [19–20]. The ability of ABCG2 to transport sulfate-conjugated phenol compounds has been previously described [5, 21]. Moreover, ABCG2 has been recently reported to be an important physiological mediator of phenolic conjugation [22]. In the same study, Zhu *et al.* demonstrated that both sulfotransferase activity and ABCG2-mediated efflux of sulfate conjugates are saturable processes. Our previous findings, showing that administration of a non-selective SULT1 inhibitor increases the entry of URB937 into the brain [3], suggest that this compound might be a substrate for SULT1 activity. Further experimentation is needed, however, to conclusively test this hypothesis.

Significant synthetic efforts have been directed at targeting ABC-transporters, to develop compounds that are either able to circumvent transport-mediated resistance (e.g. in chemotherapy) or show improved bioavailability and therapeutic index through specific transporter recognition [20, 23–24]. The present results indicate that ABCG2 is responsible for the extrusion of URB937 from the CNS. This finding provides the structural information needed to discover novel peripherally restricted FAAH inhibitors devoid of central side effects.

Acknowledgments

The authors thank Dr. A.H. Schinkel (The Netherlands Cancer Institute, Amsterdam, The Netherlands) who provided MDCK cells and their transduced cell lines, and Abcg2 knockout mice. This study was partially supported by grants from the National Institutes on Drug Abuse (RO1-DA-012413 to D.P.) and the Spanish Ministry of Science and Technology (AGL2009-11730 to G.M.), predoctoral fellowship (FPU) (to B.B.) and Ramon y Cajal fellowship (European Social Fund to GM). The contribution of the Agilent Technologies/UCI Analytical Discovery Facility, Center for Drug Discovery is gratefully acknowledged.

Abbreviations

FAAH	Fatty-acid amide hydrolase
CNS	central nervous system
BCRP/ABCG2	Breast cancer resistance protein
Pgp/ABCB1	P-glycoprotein
MDCKII	Madin-Darby canine kidney
ABC	ATP-binding cassette
SULT1	phenol sulfotransferases
i.p.	intraperitoneal
s.c.	subcutaneous

References

1. Cravatt BF, Giang DK, Mayfield SP, Boger DL, Lerner RA, Gilula NB. Molecular characterization of an enzyme that degrades neuromodulatory fatty-acid amides. Nature. 1996; 384:83–87. [PubMed: 8900284]
2. Ahn K, McKinney MK, Cravatt BF. Enzymatic pathways that regulate endocannabinoid signaling in the nervous system. Chem Rev. 2008; 108:1687–1707. [PubMed: 18429637]
3. Clapper JR, Moreno-Sanz G, Russo R, Guijarro A, Vacondio F, Duranti A, et al. Anandamide suppresses pain initiation through a peripheral endocannabinoid mechanism. Nat Neurosci. 2010; 13:1265–1270. [PubMed: 20852626]
4. Doyle LA, Yang W, Abruzzo LV, Krogmann T, Gao Y, Rishi AK, et al. A multidrug resistance transporter from human MCF-7 breast cancer cells. Proc Natl Acad Sci U S A. 1998; 95:15665–15670. [PubMed: 9861027]
5. Mao Q, Unadkat JD. Role of the breast cancer resistance protein (ABCG2) in drug transport. AAPS J. 2005; 7:E118–E133. [PubMed: 16146333]
6. Polgar O, Robey RW, Bates SE. ABCG2: structure, function and role in drug response. Expert Opin Drug Metab Toxicol. 2008; 4:1–15. [PubMed: 18370855]
7. Van Herwaarden AE, Schinkel AH. The function of breast cancer resistance protein in epithelial barriers, stem cells and milk secretion of drugs and xenotoxins. Trends Pharmacol Sci. 2006; 27:10–16. [PubMed: 16337280]
8. Allen JD, van Loevezijn A, Lakhai JM, van der Valk M, van Tellingen O, Reid G, et al. Potent and specific inhibition of the breast cancer resistance protein multidrug transporter in vitro and in mouse intestine by a novel analogue of fumitremorgin C. Mol Cancer Ther. 2002; 1(6):417–425. [PubMed: 12477054]
9. Jonker JW, Smit JW, Brinkhuis RF, Maliepaard M, Beijnen JH, Schellens JH, et al. Role of breast cancer resistance protein in the bioavailability and fetal penetration of topotecan. J Natl Cancer Inst. 2000; 92:1651–1656. [PubMed: 11036110]
10. Pavek P, Merino G, Wagenaar E, Bolscher E, Novotna M, Jonker JW, et al. Human breast cancer resistance protein: interactions with steroid drugs, hormones, the dietary carcinogen 2-amino-1-methyl-6-phenylimidazo(4,5-b)pyridine, and transport of cimetidine. J Pharmacol Exp Ther. 2005; 312:144–152. [PubMed: 15365089]
11. Huisman MT, Smit JW, Wiltshire HR, Hoetelmans RM, Beijnen JH, Schinkel AH. P-glycoprotein limits oral availability, brain, and fetal penetration of saquinavir even with high doses of ritonavir. Mol Pharmacol. 2001; 59:806–813. [PubMed: 11259625]
12. Huisman MT, Chhatta AA, van Tellingen O, Beijnen JH, Schinkel AH. MRP2 (ABCC2) transports taxanes and confers paclitaxel resistance and both processes are stimulated by probenecid. Int J Cancer. 2005; 116:824–829. [PubMed: 15849751]

13. Zhang Y, Wang H, Unadkat JD, Mao Q. Breast cancer resistance protein 1 limits fetal distribution of nitrofurantoin in the pregnant mouse. Drug Metab Dispos. 2007; 35:2154–2158. [PubMed: 17785426]

14. Zhou L, Naraharisetti SB, Wang H, Unadkat JD, Hebert MF, Mao Q. The breast cancer resistance protein (Bcrp1/Abcg2) limits fetal distribution of glyburide in the pregnant mouse: an Obstetric-Fetal Pharmacology Research Unit Network and University of Washington Specialized Center of Research Study. Mol Pharmacol. 2008; 73:949–959. [PubMed: 18079276]

15. Real R, Egido E, Perez M, Gonzalez-Lobato L, Barrera B, Prieto JG, et al. Involvement of breast cancer resistance protein (BCRP/ABCG2) in the secretion of danofloxacin into milk: interaction with ivermectin. J Vet Pharmacol Ther. 2010

16. Tang SC, Lagas JS, Lankheet NA, Poller B, Hillebrand MJ, Rosing H, et al. Brain accumulation of sunitinib is restricted by P-glycoprotein (ABCB1) and breast cancer resistance protein (ABCG2) and can be enhanced by oral elacridar and sunitinib coadministration. Int J Cancer. 2011

17. Robey RW, To KK, Polgar O, Dohse M, Fetsch P, Dean M, et al. ABCG2: a perspective. Adv Drug Deliv Rev. 2009; 61:3–13. [PubMed: 19135109]

18. Vlaming ML, Lagas JS, Schinkel AH. Physiological and pharmacological roles of ABCG2 (BCRP): recent findings in Abcg2 knockout mice. Adv Drug Deliv Rev. 2009; 61:14–25. [PubMed: 19118589]

19. Enokizono J, Kusuhara H, Sugiyama Y. Regional expression and activity of breast cancer resistance protein (Bcrp/Abcg2) in mouse intestine: overlapping distribution with sulfotransferases. Drug Metab Dispos. 2007; 35:922–928. [PubMed: 17353350]

20. Giacomini KM, Huang SM, Tweedie DJ, Benet LZ, Brouwer KL, Chu X, et al. Membrane transporters in drug development. Nat Rev Drug Discov. 2010; 9:215–236. [PubMed: 20190787]

21. Imai Y, Asada S, Tsukahara S, Ishikawa E, Tsuruo T, Sugimoto Y. Breast cancer resistance protein exports sulfated estrogens but not free estrogens. Mol Pharmacol. 2003; 64:610–618. [PubMed: 12920197]

22. Zhu W, Xu H, Wang SW, Hu M. Breast cancer resistance protein (BCRP) and sulfotransferases contribute significantly to the disposition of genistein in mouse intestine. AAPS J. 2010; 12:525–536. [PubMed: 20582579]

23. Nakagawa H, Saito H, Ikegami Y, Aida-Hyugaji S, Sawada S, Ishikawa T. Molecular modeling of new camptothecin analogues to circumvent ABCG2-mediated drug resistance in cancer. Cancer Lett. 2006; 234:81–89. [PubMed: 16309825]

24. Pick A, Muller H, Mayer R, Haenisch B, Pajeva IK, Weigt M, et al. Structure-activity relationships of flavonoids as inhibitors of breast cancer resistance protein (BCRP). Bioorg Med Chem. 2011; 19(6):2090–2102. [PubMed: 21354800]

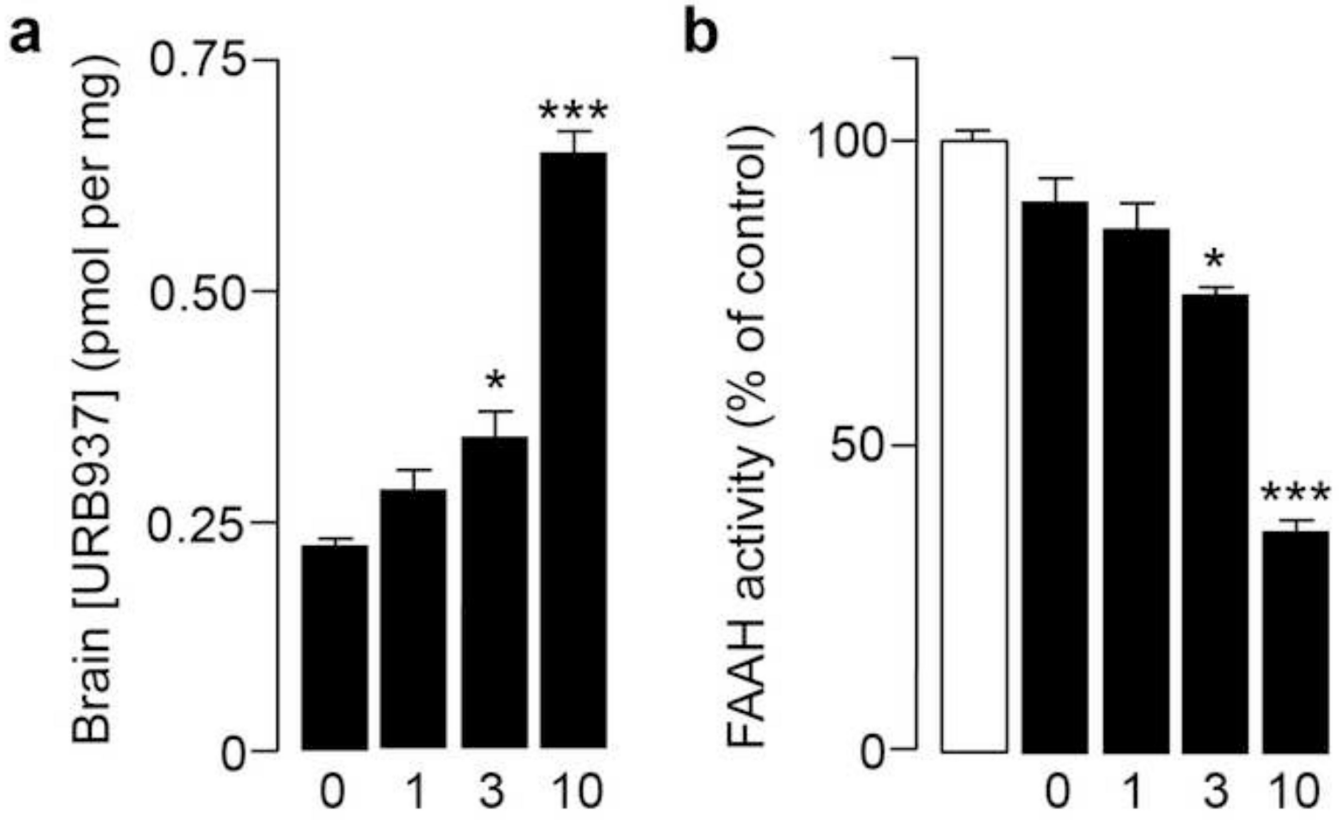

Figure 1. Effects of the selective ABCG2 inhibitor Ko143 on URB937 access to brain in mice

Intraperitoneal administration of Ko143 (0, 1, 3 and 10 mg-kg^{-1}) (a) increases the levels of URB937 (administered at 25 mg-kg^{-1}, s.c.) in mouse brain tissue; and (b) allows URB937 to inhibit brain FAAH activity. *$P < 0.05$; ***$P < 0.001$ *vs.* vehicle-treated animals; ANOVA with Dunnett's *post hoc* test; $n = 4$. Data are expressed as mean ± SEM.

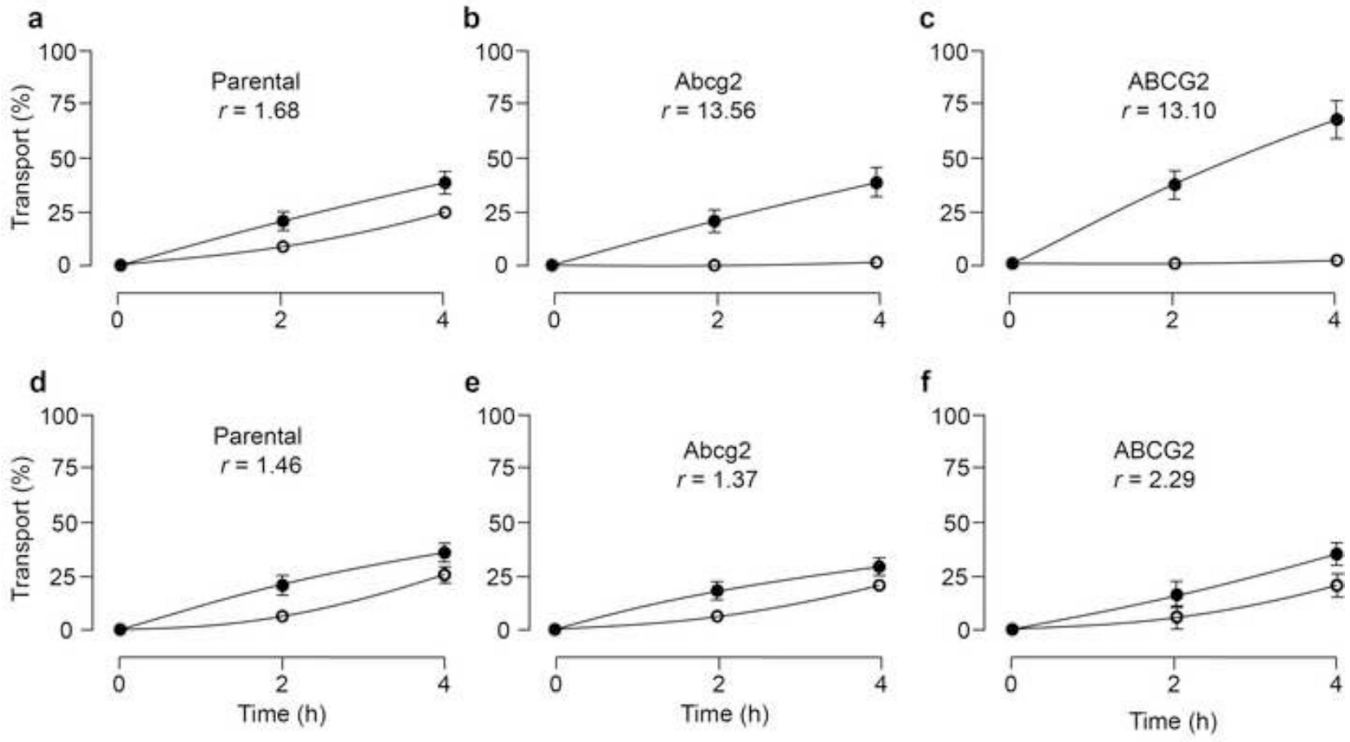

Figure 2. Transepithelial transport of URB937

Transport of URB937 (5 μM) in MDCK-II parent (a), MDCKII-Abcg2 (b), and MDCK-II-ABCG2 (c) monolayers. The experiment was started with the addition of URB937 to one compartment (basolateral or apical). After 2 and 4 h, the percentage of drug appearing in the opposite compartment was measured by HPLC/MS and plotted. ABCG2 inhibitor Ko143 (1μM) (d, e and f) was present as indicated. Results are means; error bars (sometimes smaller than the symbols) indicate S.D. ($n = 3$). ●, translocation from the basolateral to the apical compartment; ○, translocation from the apical to the basolateral compartment. *r* represents the relative transport ratio (apically direct transport divided by the basolaterally directed translocation) at t = 4h.

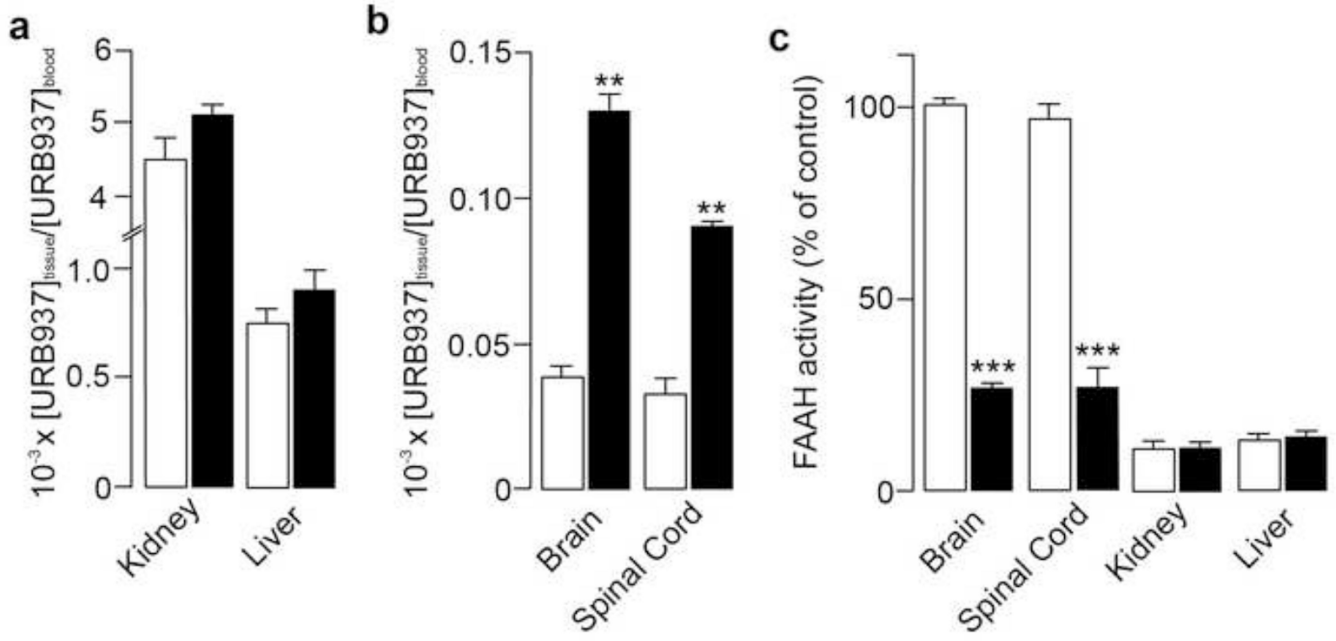

Figure 3. Effects of URB937 in Abcg2$^{-/-}$ mice

Panels a and b show the ratio between tissue and plasma levels of URB937 1 h after administration of URB937 (25 mg-kg^{-1}, s.c.) in wild-type (open bars) and Abcg2$^{-/-}$ mice (filled bars). Ablation of Abcg2 had no effect on the distribution of URB937 in peripheral tissues (a), but significantly increased CNS permeability of the compound (b). Furthermore, URB937 (25 mg-kg^{-1}, s.c.) abolished FAAH activity after 1 h in peripheral tissues of both Abcg2$^{-/-}$ and wild-type mice (c). Brain FAAH activity is not affected in wild-type mice, but is strongly reduced in Abcg2$^{-/-}$ mutants (c). $^{**}P < 0.01$; $^{***}P < 0.001$ *vs.* wild-type littermates; Student's *t*-test; $n = 4–5$. Data are expressed as mean ± SEM.

Table 1

Levels of URB937 in plasma, peripheral tissues and CNS of wild-type and Abcg2$^{-/-}$ mice measured 1 h after systemic administration (25 mg-kg^{-1}, s.c.).

Genotype/ tissue	Plasma (pmol/μL)	Liver (pmol/mg)	Kidney (pmol/mg)	Brain (pmol/mg)	Spinal Cord (pmol/mg)
Wild-type	8.34 ± 1.7	7.51 ± 3.1	33.88 ± 3.3	0.46 ± 0.12	0.29 ± 0.04
Abcg2$^{-/-}$	6.95 ± 0.9	7.75 ± 2.3	34.97 ± 0.35	1.15 ± 0.04 *	0.80 ± 0.10 *

* $P < 0.05$ *vs.* wild-type littermates; Student *t*-test; $n = 4–5$. Data are expressed as mean ± SEM.